Mixing of Viscous Non-Newtonian Fluids in Packed Beds

H. L. HASSELL and ARNOLD BONDI

Shell Development Company, Emeryville, California

Radial mixing of concentrated solutions of rubber dissolved in a light aliphatic hydrocarbon was studied in beds packed with glass spheres or York mats. The degree of mixing in the bed of spheres was significantly better, that is the Peclet number much smaller, than predicted from Wilhelm's correlation.

Pressure drop associated with the flow of rubber cement through packed beds is well represented by existing correlations, provided the effective viscosity is obtained from a shear rate vs. shear stress diagram for the fluid.

Tracer-tagged, concentrated solutions of rubber dissolved in a light aliphatic hydrocarbon ("rubber cement") were mixed in beds packed with glass spheres or with York mats. Radial mixing was determined by a concentration traverse at the bed surface. The degree of mixing in the bed of glass spheres was significantly better, that is the Peclet number significantly smaller, than predicted from Wilhelm's correlation. Power requirements for mixing equiviscous solutions in a bed of York mats compares favorably with those in stirring devices. The method is unsuited for mixing viscous with nonviscous solution because of the well-known tendency for fingering or channelling.

The pressure drop for the flow of rubber cement through packed beds is well represented by existing correlations, provided the effective viscosity is obtained from a shear rate vs. shear stress diagram for the fluid. A procedure for doing this is described.

PURPOSE AND SCOPE

The present work was undertaken to ascertain whether packed beds could be used for the mixing of very viscous non-Newtonian fluids, and, if so, how the mixing efficiency and pressure drop could be calculated. While it was clear from the outset that high form drag would prohibit the use of all but very open mesh packings, a few experiments with glass spheres were carried out to establish contact with known and reasonably well-understood principles of radial mixing in packed beds.

The polymer solutions used in this work were characterized more extensively than ordinary liquids in order to make the results suitable for extrapolation to other systems. A method had to be devised to estimate the effective shear stress and thus the effective viscosity in the bed. Owing to circumstances beyond the authors' control, the polymer solutions were less non-Newtonian than expected, making the data somewhat less valuable for extrapolation than they might have been otherwise.

RESULTS OF MIXING EXPERIMENTS

In the apparatus described, a benzene-tagged rubber solution (solvent viscosity = 0.21 centipoise) was injected from a point source in the center of a cylindrical stream of untagged rubber solution moving at equal speed upward through a packed bed. The benzene concentration traverse at the upper end of the bed provided the measurement of mixing quality. With the method of Bernard and Wilhelm (*1*) used for evaluation, the radial mixing data are expressed in terms of the effective eddy diffusivity E.

THE GLASS-SPHERE PACKING

Mixing in a bed (randomly) packed with 5-mm. diameter glass spheres is plotted in Figure 1 as Peclet number $N_{Pe} = u \cdot d_p / E$ vs. Reynolds number $N_{Re} = u \cdot d_p \rho / \eta_a'$ where the effective apparent viscosity η_a' prevailing in the bed at velocity u was obtained by a method described later.

The broken lines in Figure 1 represent typical radial-dispersion behavior of liquids in packed beds, as recently proposed by Wilhelm (*2*). Region I is the mixing regime prevailing in most commercial packed bed installations. Its behavior has been successfully explained by Baron (*3*) in terms of a random-walk model. Below a certain value of N_{Re}, the filaments of liquid appear to mix less and less well, and N_{Pe} rises. However, since E is the sum of eddy diffusivity e and molecular diffusion D, N_{Pe} does not rise indefinitely. The transition region II goes through a maximum where $e \approx D$, and for slower flow rates N_{Pe} is determined by molecular diffusion. The location of the limiting curve III*a* is given by $N_{Pe}/N_{Re} = \left(\frac{\gamma}{D}\right) = N_{Sc}$, the Schmidt number, and is therefore defined just for a particular liquid system. In the case of III*a*, it is for the mixing of a dye with water. For the polymer solution system under consideration, the limiting curve may be near III*b* or higher.

Unexpectedly, the present experimental data points do not fall on a continuation of the rising branch of curve II toward line III*b*. The mixing of the polymer solutions is very much better than expected. A 10,000 fold increase in N_{Re} is required to bring the experimental points into approximate coincidence with curve II. Ten thousand is

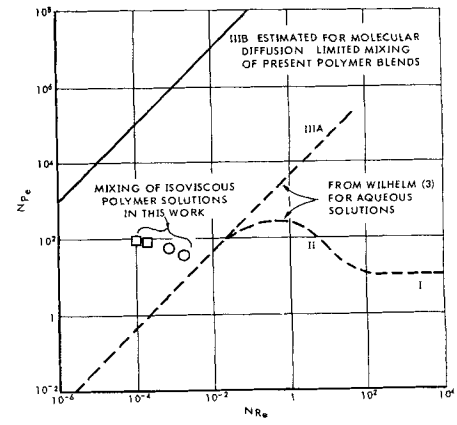

Fig. 1. Peclet number for radial dispersion in packed beds as function of Reynolds number.

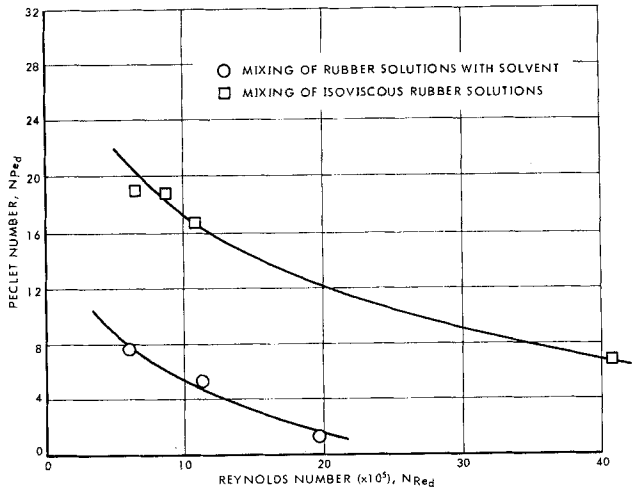

Fig. 2. Mixing characteristics of York mat mesh.

roughly the ratio of the viscosity associated with the pressure drop through the bed to the viscosity of the polymer solution prevailing at very high shear stresses, that is a small multiple of the solvent viscosity. The meaning of this observation in terms of the flow pattern in the bed is obscure at present.

YORK MAT PACKING

The packing density of York mats, commonly used as demisting equipment, is so much smaller than, and its geometry so different from, that of the glass bead packing that a direct comparison is rather difficult. Moreover, the concentration profiles obtained after mixing in the mats were often so distorted (by channelling) that the evaluation of the diffusivity E became quite uncertain. Yet, at a given pressure drop, mixing of isoviscous solutions was rather more effective than in the glass bead packing. Mixing of solvent with the polymer solution was effective in spite of very extensive channelling. The results of these experiments are presented in Figure 2.

The mixing of 200 gal./min. (as example) of two equiviscous streams of rubber cement with an 80% approach to uniformity would require a packed bed of York mats, 4 ft. in diameter, 2 ft. deep, with 120 injection nozzles on 4-in. centers. The expected pressure drop is 45 lb./sq. in., equivalent to 5 hp. In accordance with independent measurements by R. H. Overcashier (*4*) an in-line Y-stirrer mixer equires about 20 hp. to do the same mixing job. The complexity of design and its unsuitability for the mixing of thin with viscous fluids will, however, generally militate against the use of packed beds as mixing devices for thick polymer solutions.

EXPERIMENTAL DATA

The data collected consisted of shear stress-shear rate curves for the polymer solutions, pressure drops across the packed beds, radial diffusion characteristics of packs of glass spheres and York mat mesh, and inspection data on the polymer solutions. The inspection data (Table 1) were necessary because the solutions had aged, and it was felt that the aging process had probably changed the nature of the polymer. Thus, concentration, intrinsic viscosity, molecular weight, etc., were determined.

FLOW CURVES

Flow characteristics of the rubber solutions were measured over a wide range of pressure drops in a metallic capillary type of viscometer. The lower limit of shear

TABLE 1

Drum no.	Solids rubber, wt. %	Intrinsic viscosity, dl/g	Light scattering molecular weight, (X10^6)
1	17.45	8.85	4.00
2	13.58	6.18	2.35
2	15.50	6.18	2.35
2	4.59	6.18	2.35
3	12.10	5.70	2.10

stress was set by the ability to make accurate pressure-drop or flow-rate measurements, while the upper limit was determined by the capacity or pressure rating of the pumps and by a desire to avoid temperature increases in the fluid due to viscous energy dissipation. Figure 3 presents the data. Pseudo Newtonian flow is approached at both the lower and higher flow rates. It is clear from the curves that the Ostwald-deWaele flow equation, $\dot{e} = k\tau^n$, is valid only in a narrow region of flow. Hence, the often used Metzner correlations, which are based on the above equation, are of limited applicability with these solutions.

The non-Newtonian properties correlate in a manner which closely resembles a Bueche diagram (Figure 4). Bueche's theory predicts that log η_c/η_o should correlate with log $\dot{e}\eta_o/CT$ for coiling polymers (*5, 6*), where η_c is the Couette viscosity. For a true Bueche plot, the apparent viscosity η should be corrected to η_c, but since the authors' applications involve flow through channels or pipes, they have ignored the correction.

Ferry et al. (*7*) pointed out that the viscosity of many polymer solutions varies as the fifth power of the concentration. It is true for these rubber solutions. A log-log plot of the viscosity at zero shear rate against concentration for the rubber solutions having I.V. = 6.18 (that is Drum 2) is a straight line with a slope of 5. In addition, Ferry has shown that the viscosity of many polymer melts and their concentrated solutions varies as the 3.4 power of the molecular weight. It is known that the exponent of the Staudinger equation for this rubber dissolved in toluene is about 0.72 when the number average molecular weight is used. Thus, one would expect that the viscosity of these polymer solutions would vary as the 2.5 power of the intrinsic viscosity (that is 3.4 × 0.72). This is nearly true for the narrow range of intrinsic viscosities covered in

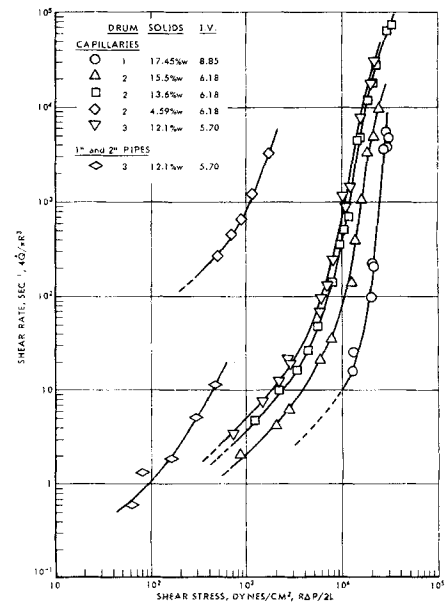

Fig. 3. Shear rate vs. shear stress for rubber solutions.

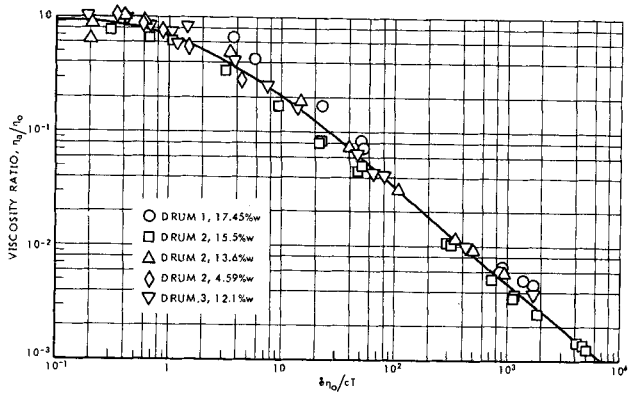

Fig. 4. Variation of viscosity with rate of shear.

these experiments; that is $\eta_o = 6.9 \times 10^{-6}\ C^5\ [\eta]^{2.5}$ fits the data very well. The deviations observed may be due to the use of a light aliphatic hydrocarbon rather than the toluene as solvent.

The flow curves (Figure 3) are, in principle, independent of the viscometric scale and should apply to pipes of any size. Accordingly, the flow characteristics through 1- and 2-in. pipes were measured. The pipe sections were 4 ft. long and had pressure taps located 6 in. from either end. The data are shown in Figure 3. Entrance and elastic deformation effects are not negligible in the pipes as they were for the capillaries; otherwise the data for Drum 3 would be on a single curve. Hence, great care must be exercised with scaling up processes which deal with viscous high polymer solutions.

FLOW IN PACKED BEDS

The packed bed data were collected in the equipment sketched in Figure 5 and are plotted in Figures 6, 7, and 8. The heart of the equipment was a 4 ft. length of either 1- or 2-in. steel pipe equipped with pressure taps 6 in. from either end. The pipes were packed with glass spheres or York mat mesh. Zenith pumps, powered by a Graham variable speed transmission, forced the feeds through the beds. In turn, the pump was fed from a 28,-gal. tank containing the feed pressured to 200 lb./sq. in. with nitrogen.

Relating observed flow resistance to flow properties in packed beds requires a parameter having the nature of an effective shear rate of the liquid. Rigorously, this is not possible. However, it was reasoned that the effective shear rate could be obtained by fitting a plot of log flow rate vs. log pressure drop for the packed beds to the log $\dot{e}$ vs. log γ curve of the same cement. The corresponding apparent viscosities were then used for the correlation of the observed pressure drop data. In this way the relation

$$t_E = \frac{\Delta P}{L^{5/2}} \left(\frac{p}{4.92}\right)^{0.170} \left(\frac{d_p}{0.30}\right)^{1.32} \times 10^{-4}$$

was obtained for the beds packed with spheres. Figure 6 is a plot of this equation. The friction factor

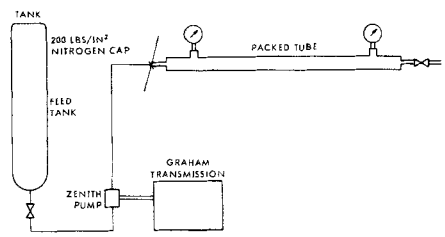

Fig. 5. Flow through packed beds.

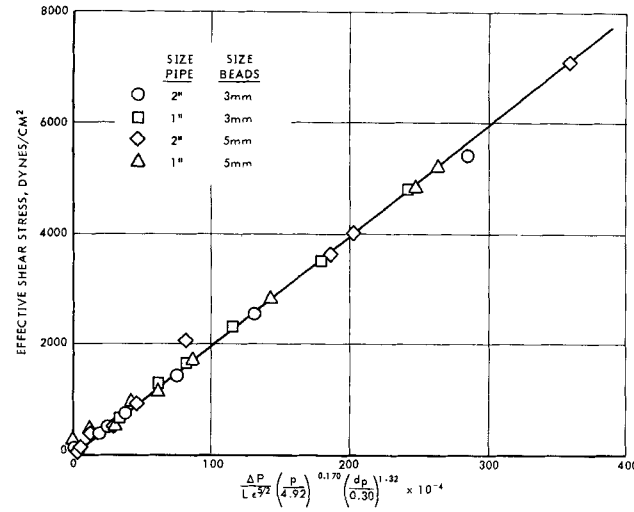

Fig. 6. Effective shear stress vs. parameters of packed bed for rubber solutions.

$$f = \frac{\Delta P\, d_p}{1/2\, \rho V^2 L}$$

with the approximate Reynolds number

$$N_{Re} = \frac{V d_p}{\eta_a}$$

produces the curves shown in Figure 7, where d_p is the diameter of the spheres and $f = 6.50/N_{Re}$. The data of Brownell et al. (8) for similar glass spheres with Newtonian fluids have been entered for comparison. The difference in behavior is small. The correlation shows that the apparent viscosities calculated by the above described method indeed determine the flow resistances through packed beds. Most of the viscosities are in the pseudo Newtonian flow region. However, the points for definitely non-Newtonian flow (all those for $N_{Re} \geq 10^{-3}$) exhibit no systematic deviation from the average curve. Nevertheless, further experimental verification will be needed before it can be said with certainty that the appropriately chosen apparent viscosity permits unique prediction of the pressure drop in laminar flow of non-Newtonian fluids through beds packed with spheres.

The friction factor for the flow of rubber solutions through York mat mesh is also a linear function of the appropriate Reynolds number (Figure 7). A difficulty here

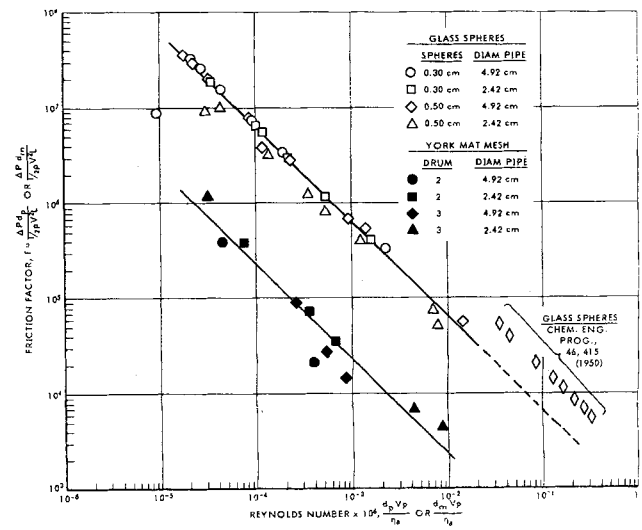

Fig. 7. Reynolds number vs. friction factor for flow of rubber solutions through porous beds.

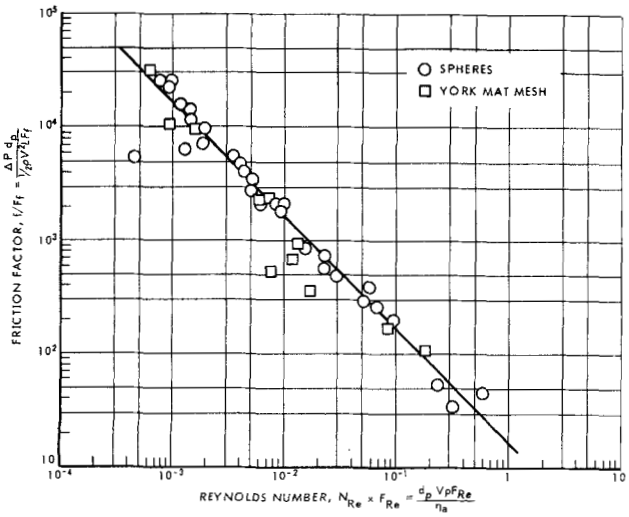

Fig. 8. Reynolds number vs. friction factor for rubber solutions through porous beds, spheres, and mesh.

is choosing the appropriate length parameter. A choice between the average mesh size or the wire diameter exits. Mesh size was taken for reasons which will be explained later. The advantage of the wire diameter is that it is a particle size and permits, in principle, making contact with other packed-bed data. This may be accomplished in the manner proposed by Brownell et al. (9), namely the introduction of a porosity correction and a particle shape factor. The porosity correction for the mesh can be made easily. However, since shape factors for mesh do not exist in the literature, the best that could be done would be to introduce an arbitrary correction factor, aside, of course, from actually determining the factor. But it was noticed that if mesh size instead of wire diameter were used to calculate the Reynolds number and friction factor, and also if the above mentioned porosity corrections were made on both the mesh and spheres, then the data for the mesh would fall on a line common with the data for the spheres (Figure 8). It should be noted here that the porosity of the York mat is changed very easily by compression. Since the pressure drop depends on $(1 - \epsilon)^8$, it is apparent that York mat data are always marred by uncertainty.

The equations which Brownell et al. suggest for spheres, and which have been used arbitrarily also for the mesh, are as follows:

$$X_e\% = 0.0316\ (100e)^{1.75}$$

$$F_{Re} = 182\ (X_e)^{-0.50}$$

$$F_f = 2.2 \times 10^6\ (X_e)^{-2.60}$$

MIXING EXPERIMENTS

The diffusion experiments were executed in the apparatus illustrated schematically in Figure 9. It consisted of a 4 ft. length of 2-in. pipe fitted at the top with five hypodermic-tubing sample ports spaced equidistant across a diameter. These constituted a traverse across the pipe. During sampling, the flow through the sample tubes was adjusted by means of valves until it was isokinetic with the main stream. The bulk of the effluent flowed through ½-in. fittings, as shown in the sketch. The sample probes extended 1 ft. into the packed bed to avoid end effects. The bottom of the packed bed had a centrally located ⅛-in. tube which could be positioned at will with respect to the sample ports. Wire spiders kept it on the center line.

The main rubber solution was fed from a 28-gal. tank to a Zenith pump which metered the flow. The ⅛-in. tube was fed from a similar setup except that the marker solution contained a small amount of benzene. The benzene profile was used as a measure of diffusion through the bed.

After a sample was taken, the light aliphatic hydrocarbon and benzene were flashed from the rubber. The solvents were analyzed by mass spectrometry to determine the benzene content. Very little benzene was needed, because the resolution of benzene in a light hydrocarbon is easily and accurately done by a mass spectrometer. This was especially important, because a large amount of marker would have altered the viscosity characteristics of the cements substantially.

The radial diffusivity was calculated from the data following the method of Bernard and Wilhelm (*1*). As suggested by these authors, the center of the profile, rather than the center of the pipe, was used to determine the radius. In a few cases, the centers coincided, but in the majority of runs, there was considerable deviation due to channelling which was extremely severe and erratic in the case of the wire mesh. The diameter used in calculating the Reynolds and Peclet numbers for the spheres was the diameter of the spheres, while in the case of the York mat mesh the average distance between strands of wire was used.

NOTATION

C = concentration, $\%_w$
d_m = mesh diameter
d_p = particle diameter
D = molecular diffusivity
e = eddy diffusivity
$\dot{e}$ = shear rate
E = effective eddy diffusivity
f = friction factor
F_f = friction factor factor
F_{Re} = Reynolds number factor
k = constant
L = length (pipe on bed)
n = exponent
N_{Pe} = Peclet number
N_{Re} = Reynolds number
N_{Sc} = Schmidt number
p = pipe diameter

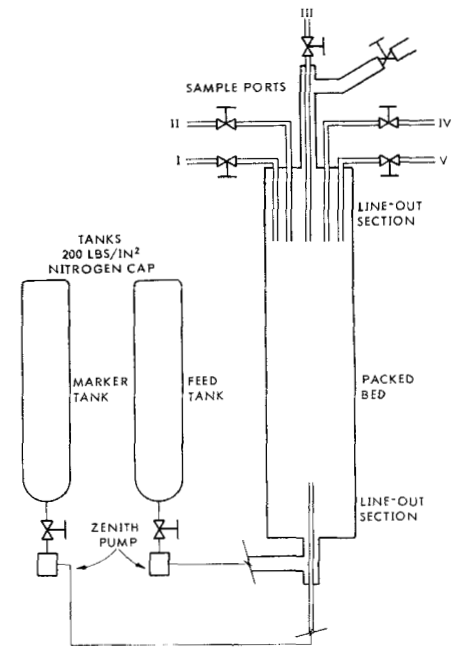

Fig. 9. Eddy diffusion equipment.

Q = volume flow rate
R = radius
T = absolute temperature
u = mean, point condition velocity in Z direction of cylindrical coordinates
V = void space velocity
X_e = effective porosity

Greek Letters

η = kinematic viscosity (η/ρ)
ϵ = fraction void space
ΔP = pressure drop
$[\eta]$ = intrinsic viscosity
η_a = apparent viscosity
η_c = Couette viscosity
η_o = viscosity at zero shear rate
η_a' = effective apparent viscosity
ρ = density
τ = shear stress
τ_E = effective shear stress

LITERATURE CITED

1. Bernard, R. A., and R. H. Wilhelm, *Chem. Eng. Progr.*, **46**, 233 (1950).
2. Wilhelm, R. H., *Pure Appl. Chem.*, **5**, 403 (1962).
3. Baron, T., *Chem. Eng. Progr.*, **48**, 118 (1952).
4. Overcashier, R. H., Private communication.
5. Bueche, F., *J. Chem. Phys.*, **22**, 1570 (1954).
6. ———, *J. Appl. Phys.*, **30**, 1114 (1959).
7. Ferry, et al., *J. Coll. Sci.*, **7**, 498 (1952).
8. Brownell, Dombrowski, and Dickey, *Chem. Eng. Progr.*, **46**, 415 (1950).
9. Brownell, L. E., et al., *A.I.Ch.E. Journal*, **2**, 79 (1956).

Manuscript received December 16, 1963; revision received July 23, 1964; paper accepted July 29, 1964.

Mixing and Chemical Reaction in Turbulent Flow Reactors

R. NORRIS KEELER, E. E. PETERSEN, and J. M. PRAUSNITZ

University of California, Berkeley, California

Mixing and a rapid, second-order irreversible chemical reaction were studied in a turbulent chemical flow reactor, with a point conductivity probe used to detect changes in concentration. From the mathematical theory of Toor, it is shown experimentally that data on the mixing of a passive scalar additive in a nonreactive system may be used accurately to predict the yield of a rapid, irreversible second-order reaction when the hydrodynamics and initial conditions on mixing for the reactive system are identical to those of the nonreactive system. Increasing the bulk average concentration of one reactant is shown to have a strong effect on the overall reaction yield.

BACKGROUND

One of the important problems of chemical engineering is prediction of fractional conversion at the outlet of a turbulent flow reactor in which the reactants are introduced and are allowed to mix and react. This problem may be rephrased in terms of chemical engineering reactor design; given the hydrodynamic or mixing properties of a flow reactor, and the kinetics of a chemical reaction, calculate the conversion accomplished in the reactor. This problem has been completely solved for a very limited number of cases, but until recently, little experimental or theoretical work has been done on the problem of simultaneous mixing and rapid chemical reaction.

Chemical reactions carried out in turbulent flow reactors can be divided into two limiting cases and one intermediate case. The two limiting cases occur when either hydrodynamics or kinetics completely dominate a combined mixing-reaction system. In the first limiting case the kinetics of the reaction are so rapid that the reaction is complete when mixing is complete. Reactions of this type are commonly called *diffusion-controlled* reactions, since the molecular diffusivity is the only reaction-limiting factor in the fine structure of the flow field. The second limiting case is the situation in which the kinetics of the chemical reaction are so slow that the reactants are completely and thoroughly mixed before any appreciable reaction has taken place. This corresponds to the most frequently encountered case in reactor design. The intermediate case, where both the hydrodynamics of mixing and the kinetics of reaction play a significant part in determining reaction yield, is interesting and becomes important in certain systems such as flame reactors. This paper considers the case of the diffusion-controlled reaction.

R. N. Keeler is presently at the Lawrence Radiation Laboratory, University of California, Livermore, California.